

# Analysis of well-log data from the White Rose oilfield, offshore Newfoundland.

Jessica Jaramillo Sarasty and Robert R. Stewart

## ABSTRACT

We used dipole sonic, density, gamma-ray, and porosity logs (density porosity and neutron porosity) in the continuing petrophysical analysis of the White Rose area, offshore Newfoundland. To this end, we have plotted seismic parameters versus various porosity measurements as determined from well logs. In general, velocity increases as total porosity decreases.  $V_p/V_s$  decreases slightly when total porosity decreases.  $V_s$  shows a high correlation with porosity. Seismic parameters show promise to predict porosity values.

In addition, we find that Castagna's "mudrock" relationship predicts  $V_s$  from  $V_p$  reasonably well in the clastic section. Better fits can be achieved by dividing the lithologies into regions.

In general, the Faust relation predicts  $V_s$  reasonably well. For a better fit with the well data it requires a constant different from 125.3, the results were encouraging.

## INTRODUCTION

We are interested in the relationship of porosity to directly observable seismic values ( $V_p$  and  $V_s$ ). In this paper our attention is focused on the White Rose oilfield, offshore Newfoundland. We used the data from well L-08 located on the South Avalon Pool (Figure 1).

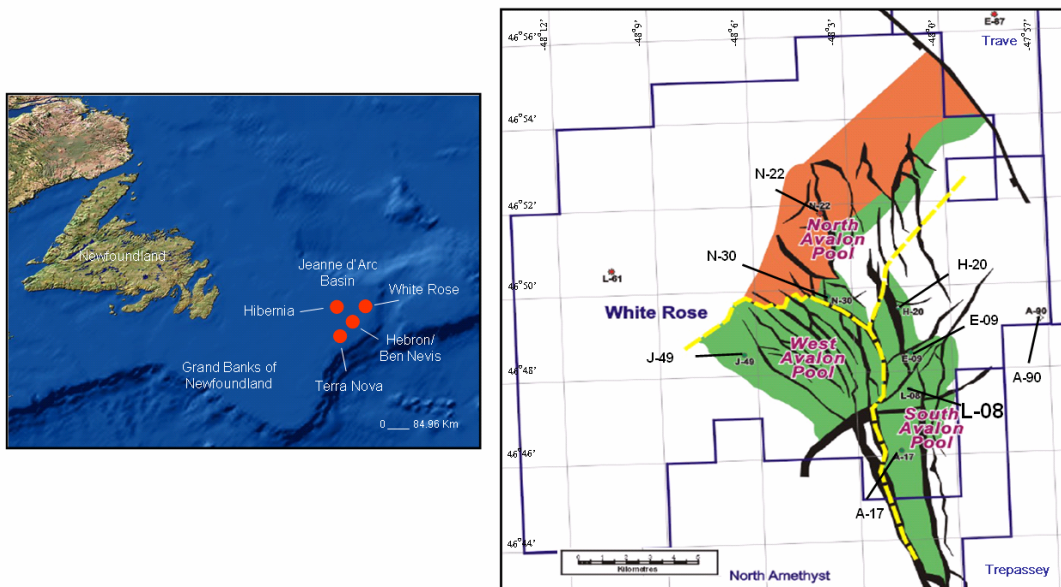


FIG. 1. The location of the White Rose oilfield and well L-08, Newfoundland. (Modified after www.GeographyNetwork.com, 2002 and Husky Energy, 2000).

The lithology encountered in this well comprises the following units (Husky Energy, 2001): The Banquereau Formation (shale), South Mara unit (glauconitic silty fine sandstone), Dawson Canyon formation (marl and calcareous shale), Petrel member (argillaceous limestone), Nautilus Formation (siltstone and shale), Avalon Formation (very fine grained sandstone, siltstone and shale), and Eastern Shoals Formation (interbedded shale, siltstone, sandstone and limestone).

Previous petrophysical analysis of the White Rose area (Jaramillo and Stewart, 2003), showed promising empirical relationships among dipole sonic, density, and gamma-ray logs. We continue the empirical analysis with porosity logs.

### WELL-LOG ANALYSIS

To be able to better understand the area of interest (Avalon sandstone) we would like to know more about the lithology and porosity of the area. One goal of the well log analysis is to understand the importance of Vs with respect to converted-wave imaging and reservoir characterization.

### Vp/Vs versus GR

To better understand well L-08 information, the results from a Vp/Vs versus GR (Figure 2) graph shows a range of data available from Nautilus, Avalon and Eastern Shoals where, as we go from shales to sandstones (decreasing GR) the Vp/Vs values decrease; in this case, the Nautilus Formation has a range of Vp/Vs between 1.98-1.62, the Avalon Formation, 2.05-1.53, and Eastern Shoals Formation, 1.85-1.77. Therefore this could make it difficult to differentiate the two lithologies based solely on Vp/Vs ratio (Jaramillo and Stewart, 2002).

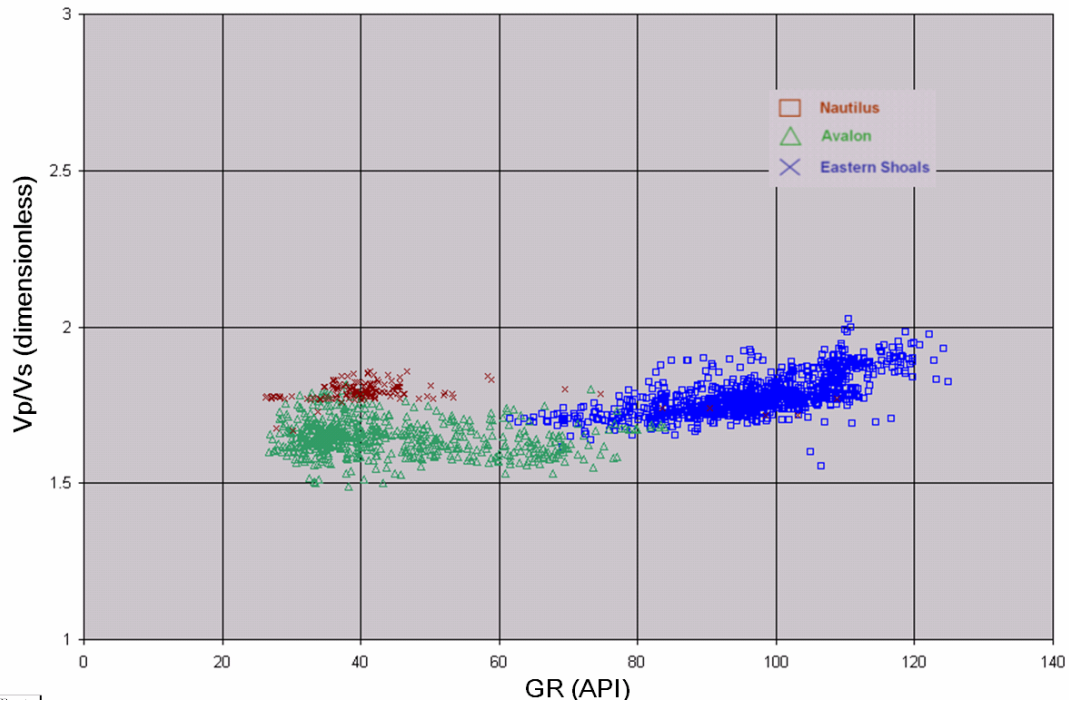


FIG. 2. The Vp/Vs versus gamma ray of well L-08

**Vp versus  $\phi_d$** 

DRHO or Delta  $\rho$  represents the correction factor applied to the  $\rho_b$  or Bulk Density in  $\text{kg/m}^3$ . Wherever Delta  $\rho$  in the log exceeds the value of  $150 \text{ kg/m}^3$  it is indicative that the skid of the density well logging tool is either not close enough to the borehole wall or is into a rough section of the borehole wall, where the density logging tool is reading a mixture of mud density and rock density. As a result, when DRHO exceeds the value of  $150 \text{ kg/m}^3$ , it indicates that a large correction factor has been applied to the Bulk density value, and therefore the bulk density value has a lower confidence level in those zones (Hilchie, 1989).

Density porosity or  $\phi_d$  is derived from the bulk density value (eqn. 1). In this case, the following equation was used:

$$\phi_d = \frac{(\rho_m - \rho_b)}{(\rho_m - \rho_f)} \quad (1)$$

Here  $\rho_m$  is the density of the matrix,  $\rho_f$  is the density of the fluid, and  $\rho_b$  is the bulk density. The density of the matrix for sandstone is  $2650 \text{ kg/m}^3$ , for limestone it is  $2710 \text{ kg/m}^3$ , and the density of the fluid is  $1000 \text{ kg/m}^3$  for fresh water. For example, when we are using density porosity in a sandstone matrix, we are referring to the transformation of bulk density into  $\phi_d$  using a value of  $2650 \text{ kg/m}^3$ .

For formations with lithologies known to be limestone (e.g. Eastern Shoals), a limestone matrix was used to derive porosity. On the other hand, for formations with lithologies known to be sandstone (e.g. Avalon), a sandstone matrix was used to derive porosity.

In cases where the matrix was sandstone (Figures 3 and 4), the total porosity increases as the velocity decreases; Banquereau and Avalon formations show a pattern with a linear regression for  $y = -1631.4x + 2943.9$ ,  $R^2 = 0.0955$  and  $y = -6846x + 5214.3$ ,  $R^2 = 0.5792$  respectively. At the top of the well there is some data that does not exhibit the same behaviour as the Banquereau shale. This could be due to problems with measurements through the casing. The Nautilus shale behaves somewhat differently from the Banquereau shale but still shows the general behaviour.

There are some negative porosity values present; these may be indicative of calcite lime in the matrix ( $2710 \text{ kg/m}^3$ ). The Vp (compressional-wave velocity) measurements are likely of various qualities which may explain some of the scattering.

For the case where the matrix was limestone (Figure 5), the behaviour was similar to the  $\phi_d$  value derived using a sandstone matrix. Eastern Shoals Formation have a linear regression where  $y = -6673.9x + 5430.9$ ,  $R^2 = 0.6135$  and for Dawson Canyon, Petrel  $y = -9470.4x + 4487.3$ ,  $R^2 = 0.3991$ . In general the velocity decreases with porosity.

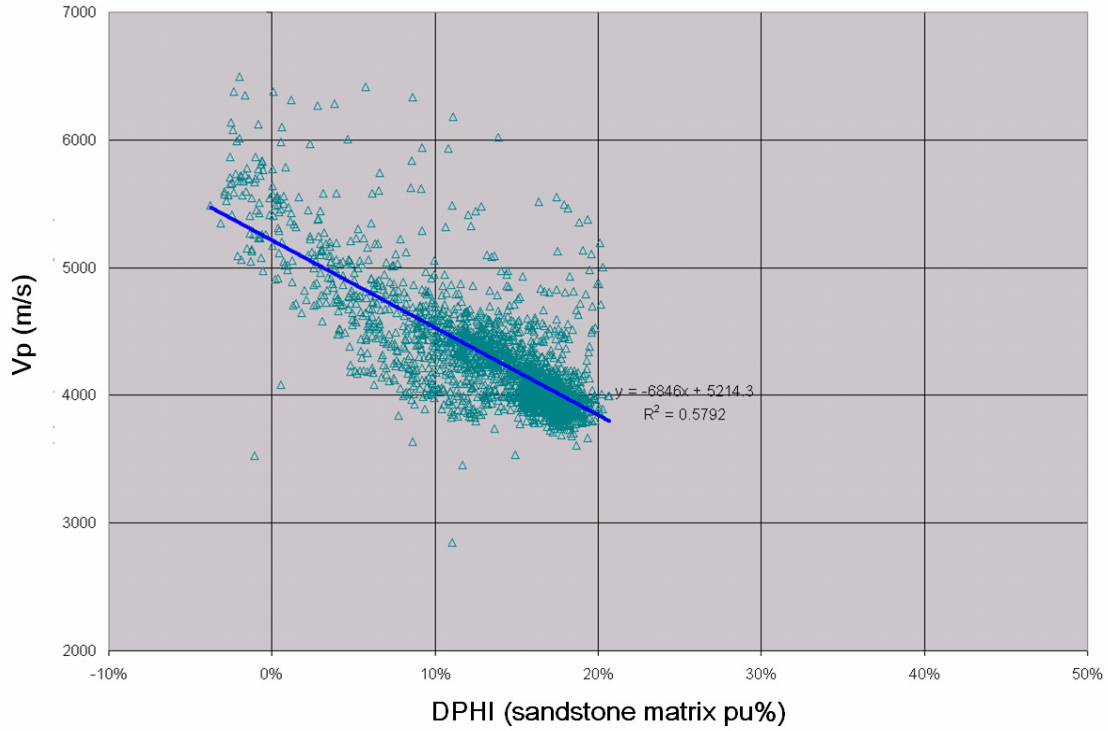


FIG. 3. Vp versus density porosity (Avalon, well L-08). All data is included in the plot, and the matrix is assumed to be sandstone.

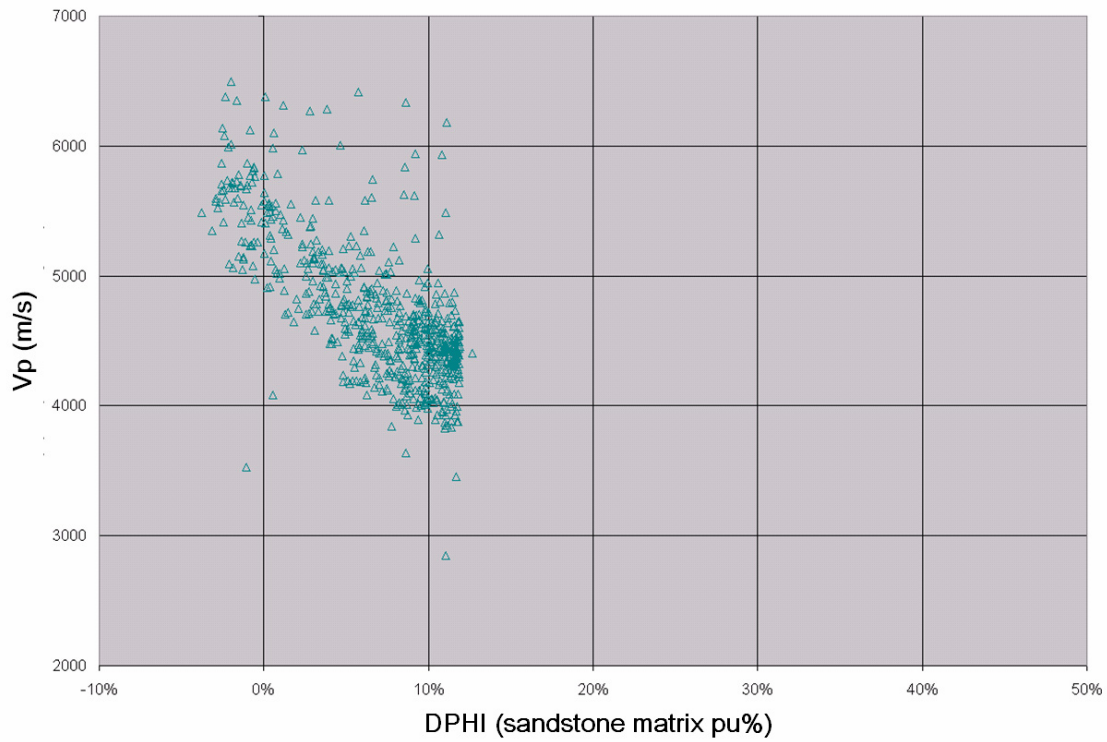


FIG. 4. Vp versus density porosity (Avalon, well L-08). The values of density porosity have a  $\Delta \rho$  no greater than  $150 \text{ kg/m}^3$ . Sandstone matrix.

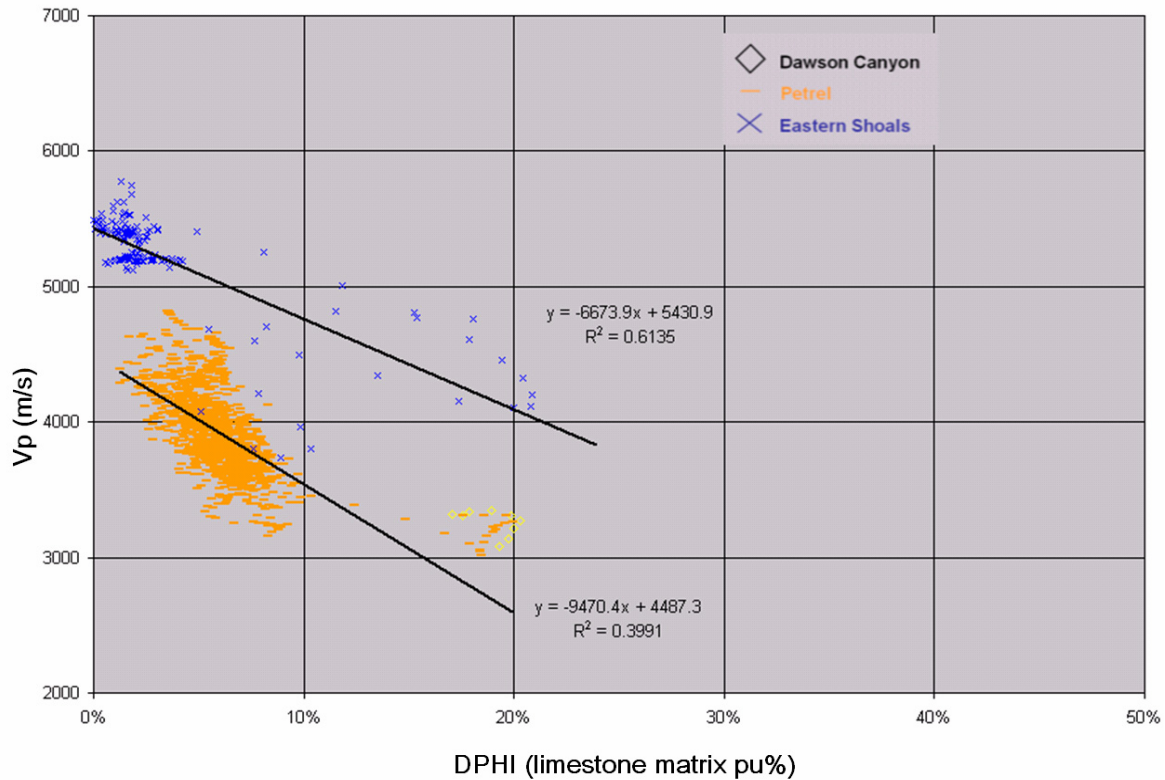


FIG. 5. Vp versus density porosity (well L-08). All data included. Assumes a limestone matrix.

### Vp versus $\phi_N$

For this relationship (Figure 6), we assumed a sandstone matrix. The general trend is a decrease of velocity when the neutron porosity increases. The general trend of the data is linear with a regression line where  $y = -10246x + 5307.9$ ,  $R^2 = 0.6057$ . The Nautilus shale is showing a high porosity value. This is unrealistic, and likely due to bound water (Hilchie, 1989).

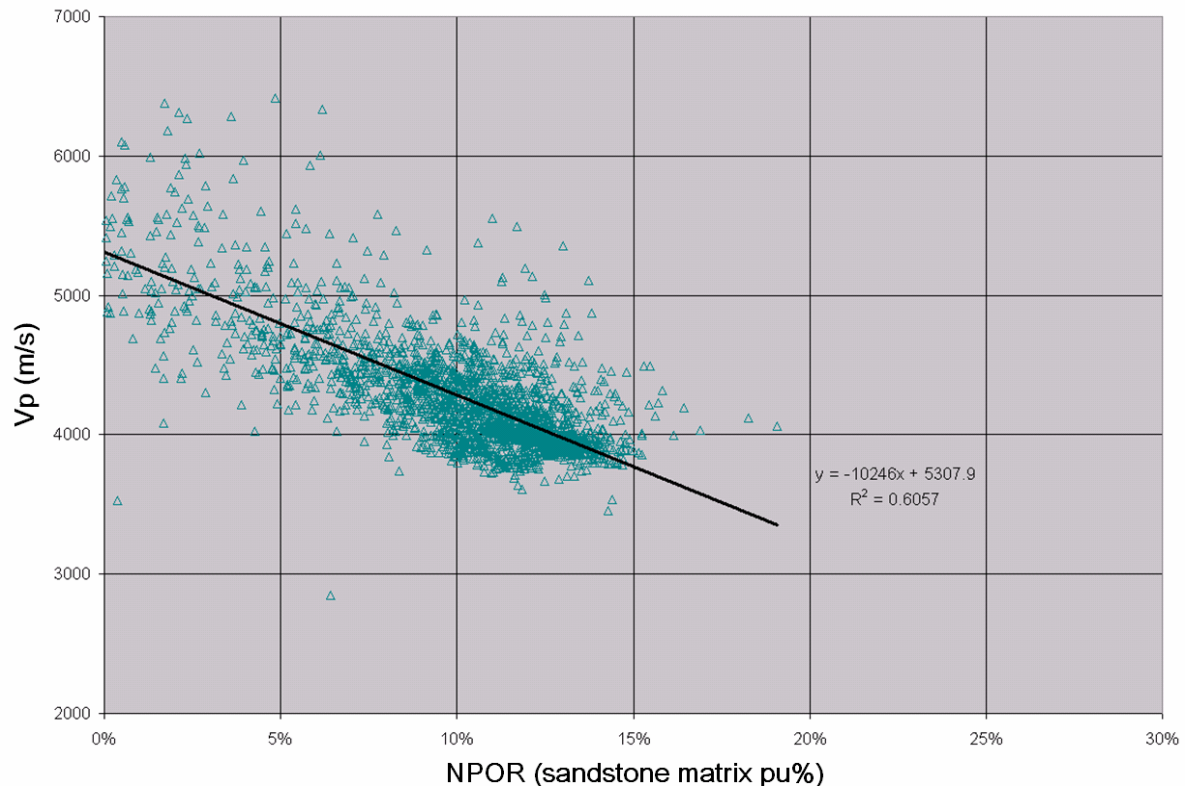


FIG. 6. Vp versus neutron porosity (Avalon, well L-08).

### Vs versus $\phi_d$

The density porosity is derived in the same manner as in the previous section (see Equation 1).

For the case where the matrix was sandstone (Figure 7), when the total porosity increases the velocity decreases. The Avalon formation shows a pattern with a linear regression for  $y = -3989.8x + 3118.8$ ,  $R^2 = 0.6854$ . The Nautilus formation exhibits a trend, but still has less velocity with high porosity. As we observed on the Vp plots, there are present some negative porosity values; these may be indicative of calcite lime in the matrix ( $2710 \text{ kg/m}^3$ ).

In the sandstone and limestone matrix case (Figure 8) the behaviour of the data is similar, and the data show a linear regression where  $y = -3066.7x + 3011.9$ ,  $R^2 = 0.534$ . In general, the velocity decreases with increasing porosity.

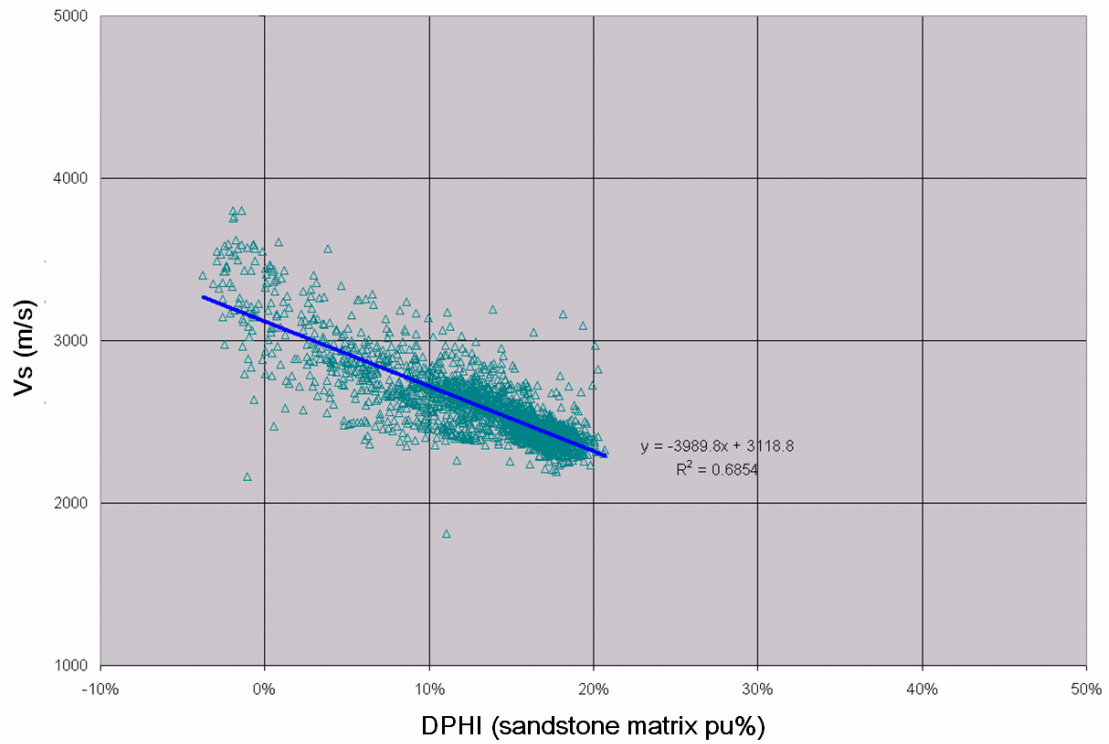


FIG. 7. Vs versus density porosity (well L-08), all data included, using a sandstone matrix.

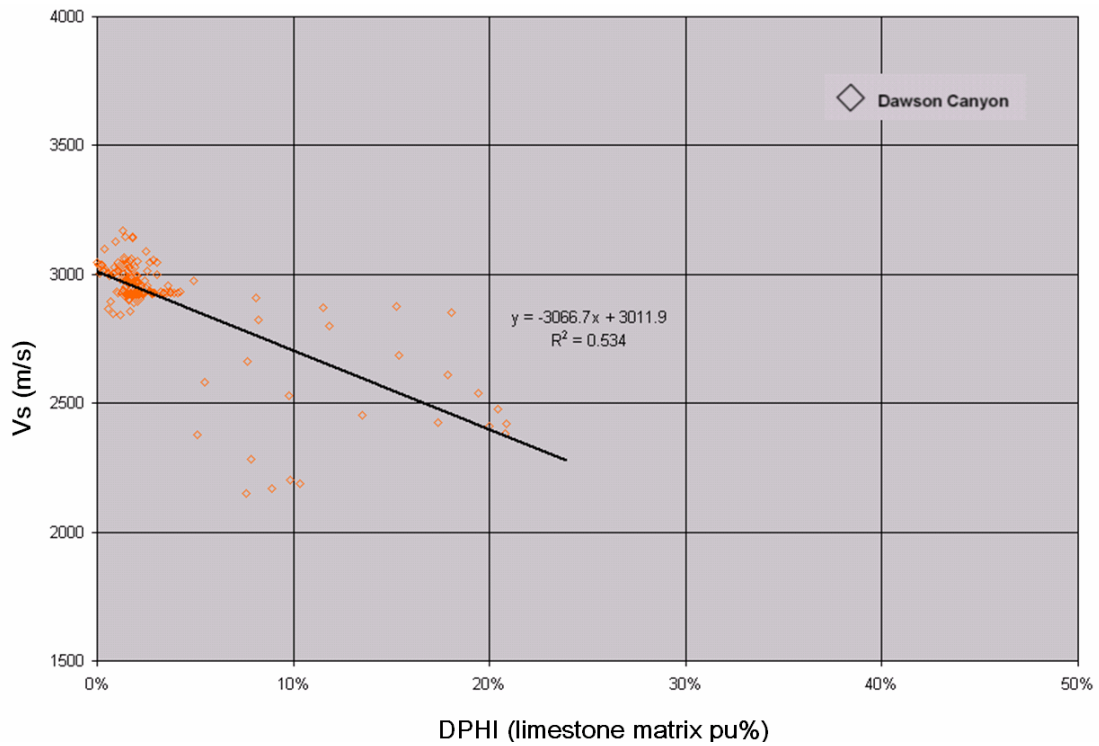


FIG. 8. Vs versus density porosity for (well L-08), all data included with a limestone matrix.

**Vs versus  $\phi_N$**

For this relationship (Figure 9), we assumed a sandstone matrix. The general trend is a decrease in velocity when the neutron porosity increases. The general trend of the Avalon data is a linear regression where  $y = -5805.2x + 3157$ ,  $R^2 = 0.6774$ . As on Vp versus  $\phi_N$ , the Nautilus shale shows high porosity values. This could be due to bound water (change in chemical composition).

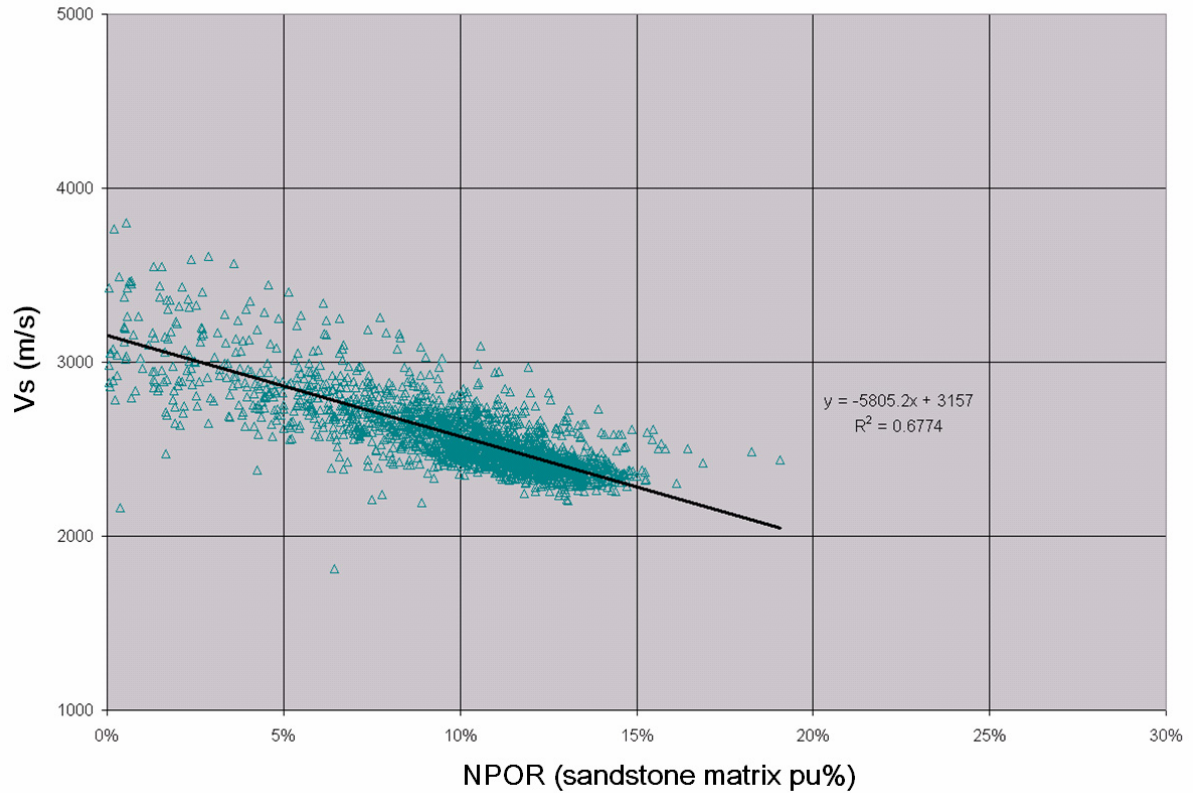


FIG. 9. Vs versus neutron porosity (Avalon, well L-08).

**Vp/Vs versus porosity**

For similar lithologies, the Vp/Vs is either unchanged or slightly increases with porosity. For limestone, Vp/Vs is unchanged for different porosity, similar to the Avalon sandstone. However for the shale an increase in porosity increases Vp/Vs. This could be caused by changes in the shale chemical composition. All the Vp/Vs are above 1.41 which is the square root of 2.

In Figure 10 (sandstone matrix) the linear regression shows  $y = -0.0716x + 1.6726$ ,  $R^2 = 0.0019$ ; the trend in the limestone matrix is  $y = -0.6557x + 1.7891$ ,  $R^2 = 0.2159$ . The Avalon Formation shows a range of Vp/Vs between 1.51-2.03. On a limestone matrix (Figure 11), the Eastern Shoals show that Vp/Vs decreases as total porosity increases.



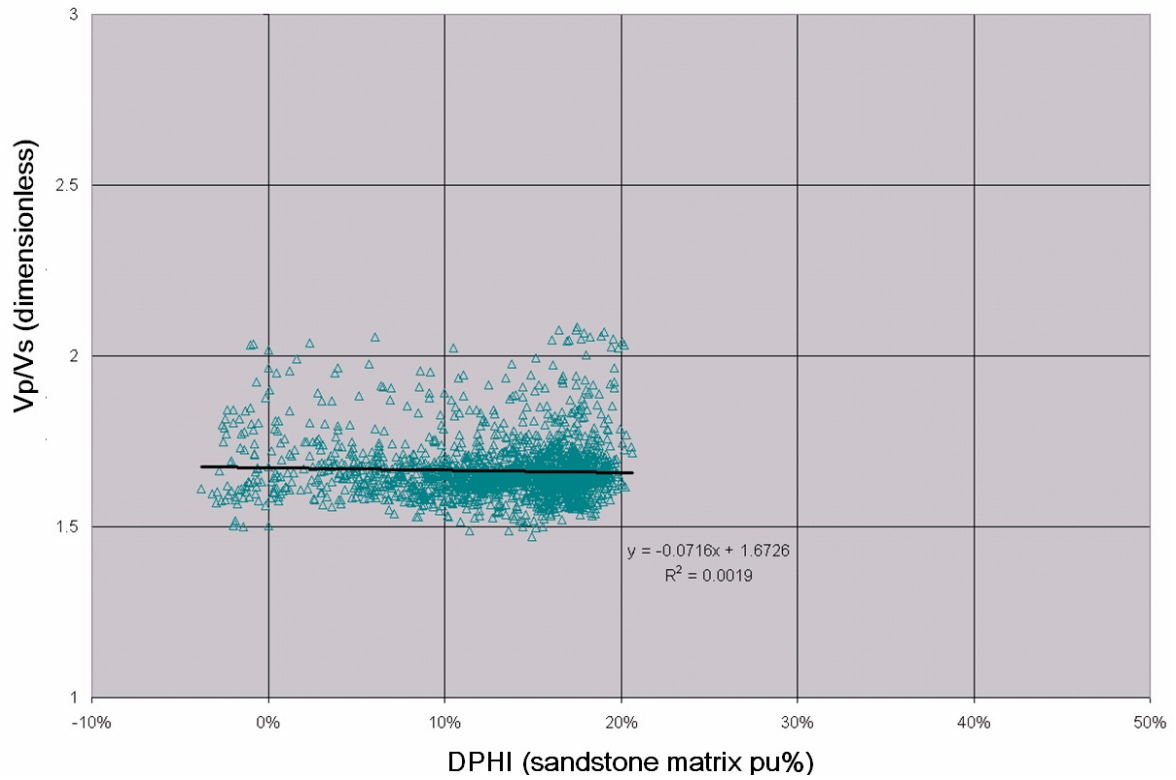


FIG. 10. Vp/Vs versus density porosity (Avalon, well L-08), including all data on a sandstone matrix.

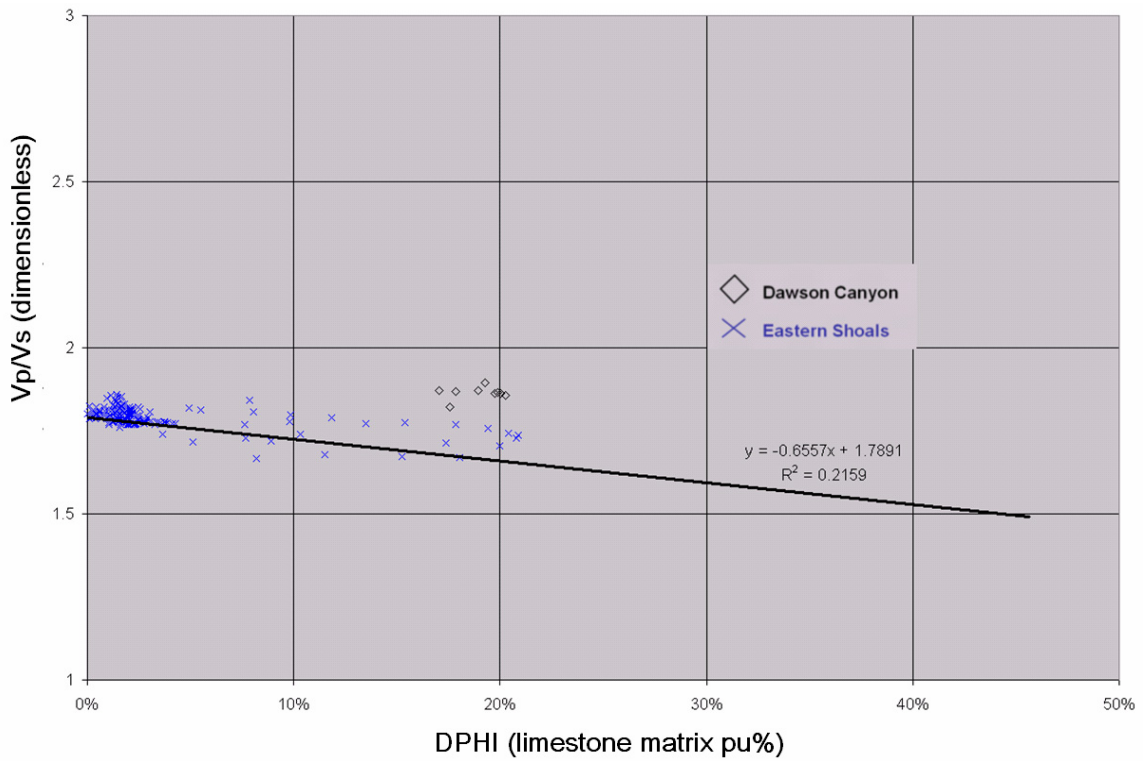


FIG. 11. Vp/Vs versus density porosity for well L-08, all data with a limestone matrix.

**Vp/Vs versus  $\phi_N$**

Vp/Vs increases when  $\phi_N$  increases for the Nautilus and the Avalon formations but for the Eastern Shoals the Vp/Vs value stays roughly the same. The general trend of the Avalon data (Figure 12), shows a linear regression of  $y = -0.2041x + 1.6831$ ,  $R^2 = 0.0074$ . The general range for Vp/Vs values for Nautilus is 1.68-1.96, Avalon, 1.51-2.04, and Eastern Shoals, 1.76-1.82.

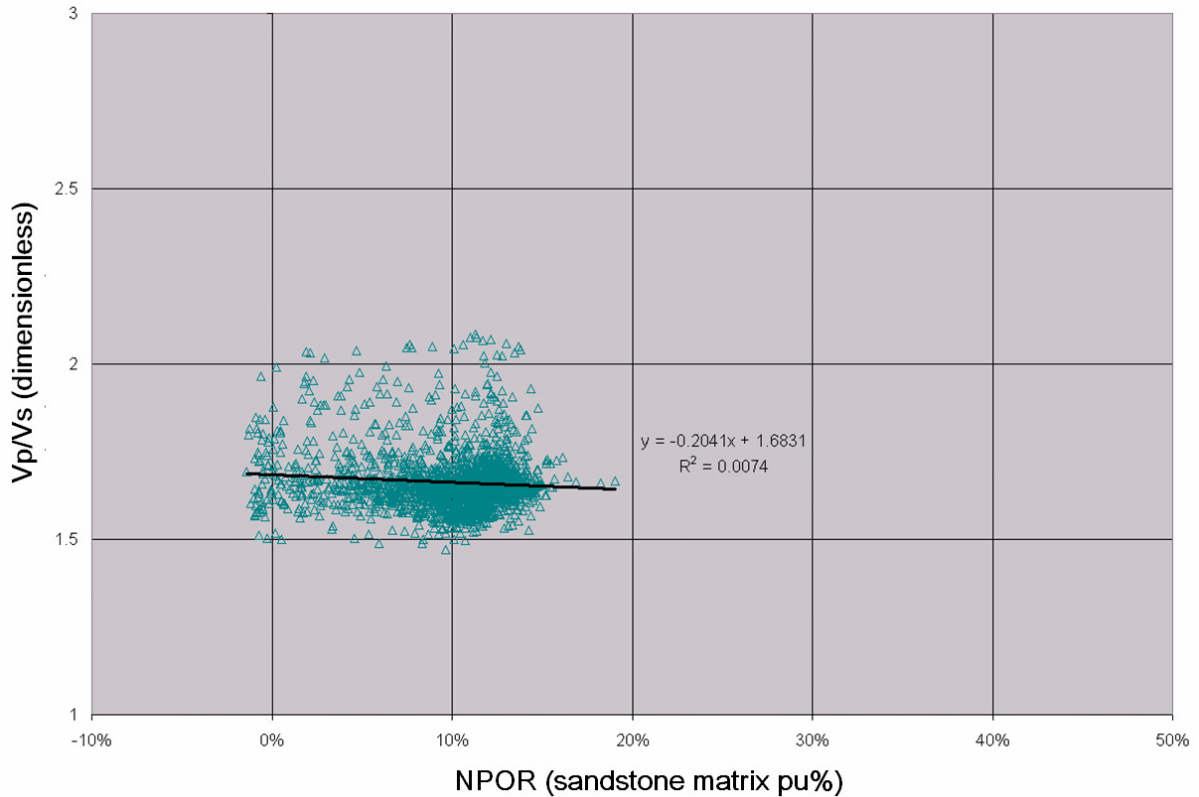


FIG. 12. Vp/Vs versus neutron porosity (Avalon, well L-08).

**$\phi_N$  versus  $\phi_d$**

Let us consider the shale effect on the density porosity versus neutron porosity cross-plot: “The introduction of noneffective shales (kaolinite and chlorite), influences the neutron log more than the density log and the cloud of data shift to higher apparent neutron porosities. This shift is, of course, wrong as the shale point should not move.” (Hilchie 1989).

At the sandstone line, there is zero percent shale. At the shale point there is 100% shale. In between, there is a series of parallel lines to the sandstone line that represent, from left to right, an increasing percentage of shale (Hilchie 1989). In Figure 13, the Nautilus shale covers that zone. It is estimated from this that the Nautilus shale ranges from 20% to 80% shales. This is consistent with the known geology of the area. The Avalon follows the sandstone line of the chart.

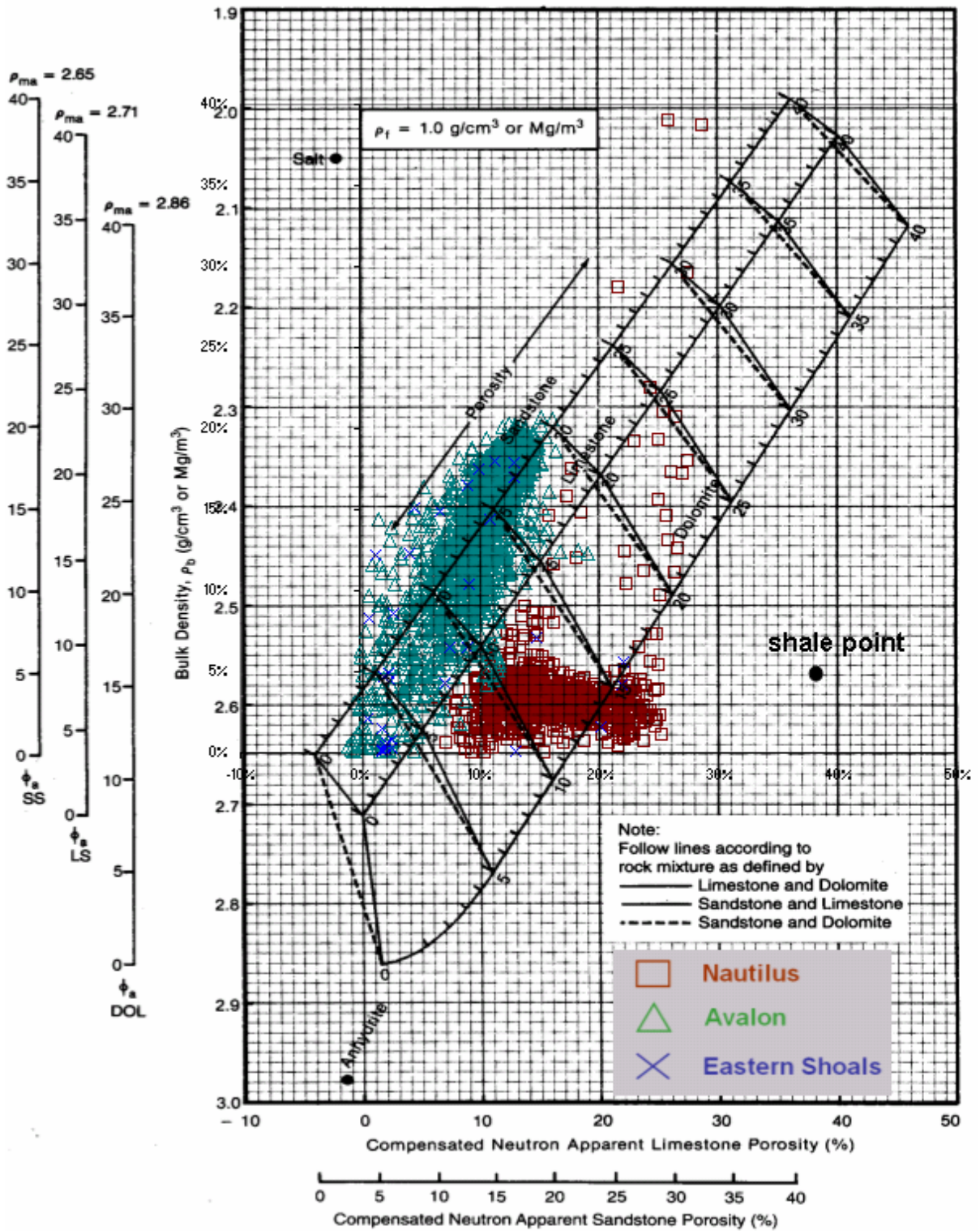


FIG. 13. Density porosity versus neutron porosity (well L-08), overlain on a chart from Western Atlas (1992).

Figure 14, shows the linear regressions from the Nautilus ( $y = 0.2777x - 0.0104$ ,  $R^2 = 0.1013$ ) and Avalon ( $y = 1.2417x + 0.0113$ ,  $R^2 = 0.7198$ ) formations. The Nautilus shale  $\phi_N$  increases when  $\phi_d$  increases; for Avalon the  $\phi_N$  increases with a steady  $\phi_d$ . As we can observe in Figure 13 the Avalon follows the sandstone line of the chart.

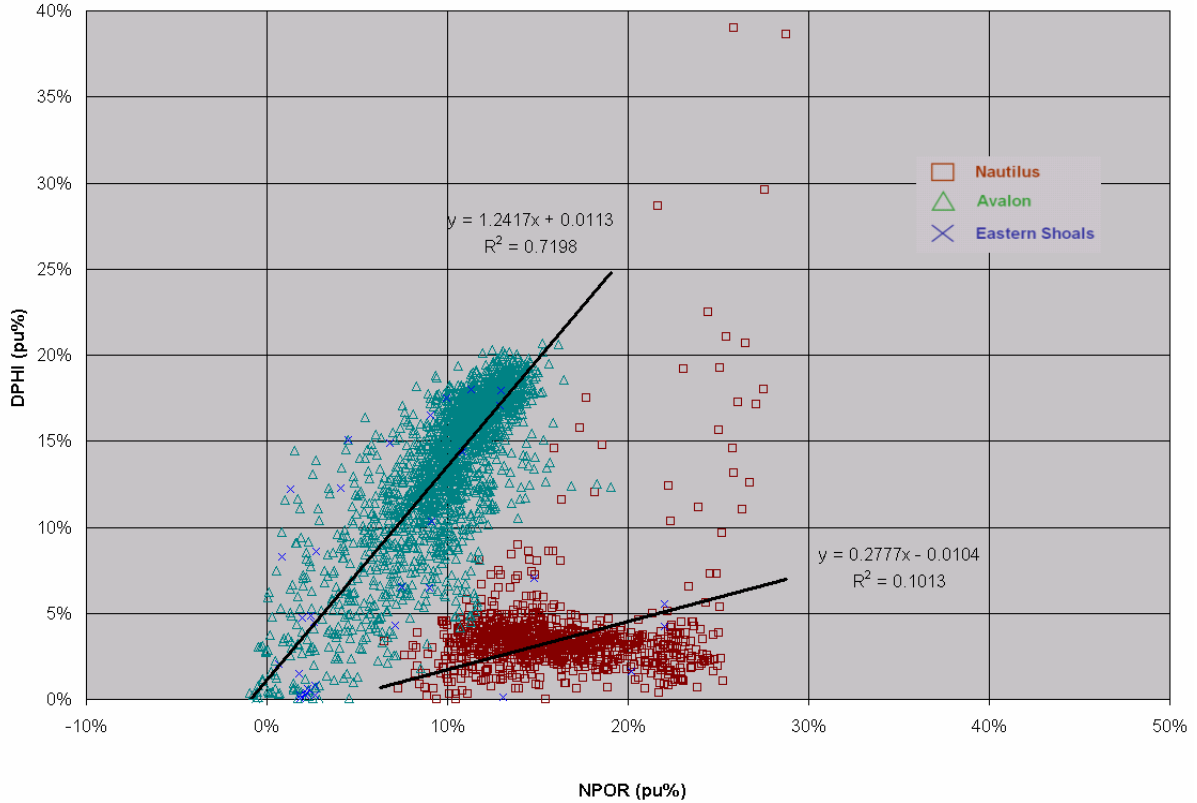


FIG. 14. Density porosity versus neutron porosity (well L-08).

### Vp/Vs versus depth

In general, Vp/Vs decreases with depth. Vp/Vs is, however, fairly constant over the Avalon interval. An overall Avalon Formation value for Vp/Vs (for siltstone and sandstone units together) is 1.65 (Figure 15).

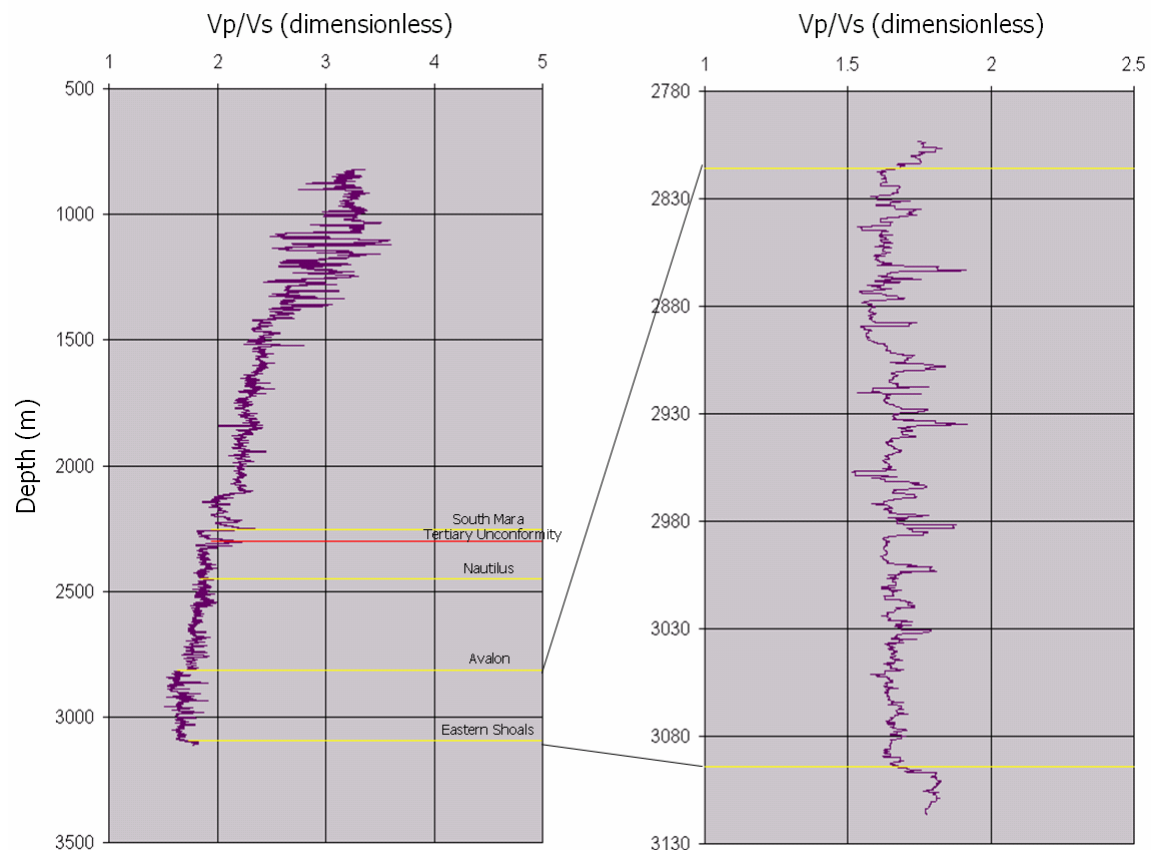


FIG. 15. Vp/Vs ratio versus depth. Well L-08 (left) and Avalon formation from well L-08 (right).

### Vs real versus Vs Faust

We explore the prediction of Vs using a relationship similar to the one used to predict Vp by Faust (1951). In this case, the “Vs Faust equation” attempts to predict shear velocities with geological time and depth of burial of the rock. The constant however is naturally quite different than 125.3. We explore this relation in wells H-20 and L-08 where the Vs was acquired. For well L-08, the fit was using a  $k$  of 81 (Figure 16).

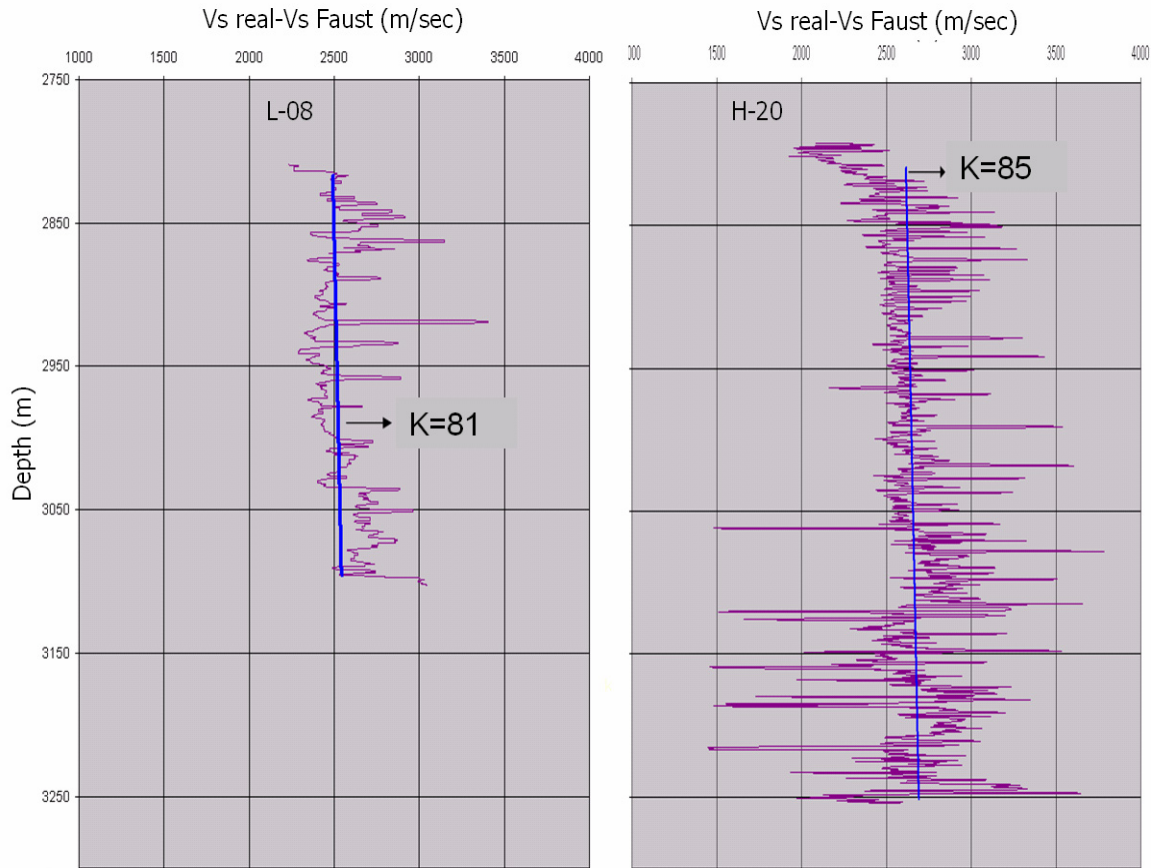


FIG.16. Vs real and Vs Faust versus depth (wells L-08 and H-20), for the Avalon unit.

### Vs real versus Vs Castagna

We used Castagna's (1985) relationship [ $V_s = (V_p - 1360) / 1.16$ ], to predict  $V_s$  from  $V_p$ . This equation predicted  $V_s$  for the entire well section fairly well. We note that this could be applied only for wells H-20 and L-08 where the real values of  $V_s$  were acquired, Figure 18 shows the prediction for the Avalon portion. The reason for the quality of fit is probably due to the fact that the lithologies in the well are mostly clastics. The results show a 10% error of prediction above and below the original  $V_s$  curve for both wells (Figure 17). Castagna experiences difficulty predicting  $V_s$  in the limestone zone of the wells H-20 and L-08 (Eastern Shoals Formation).

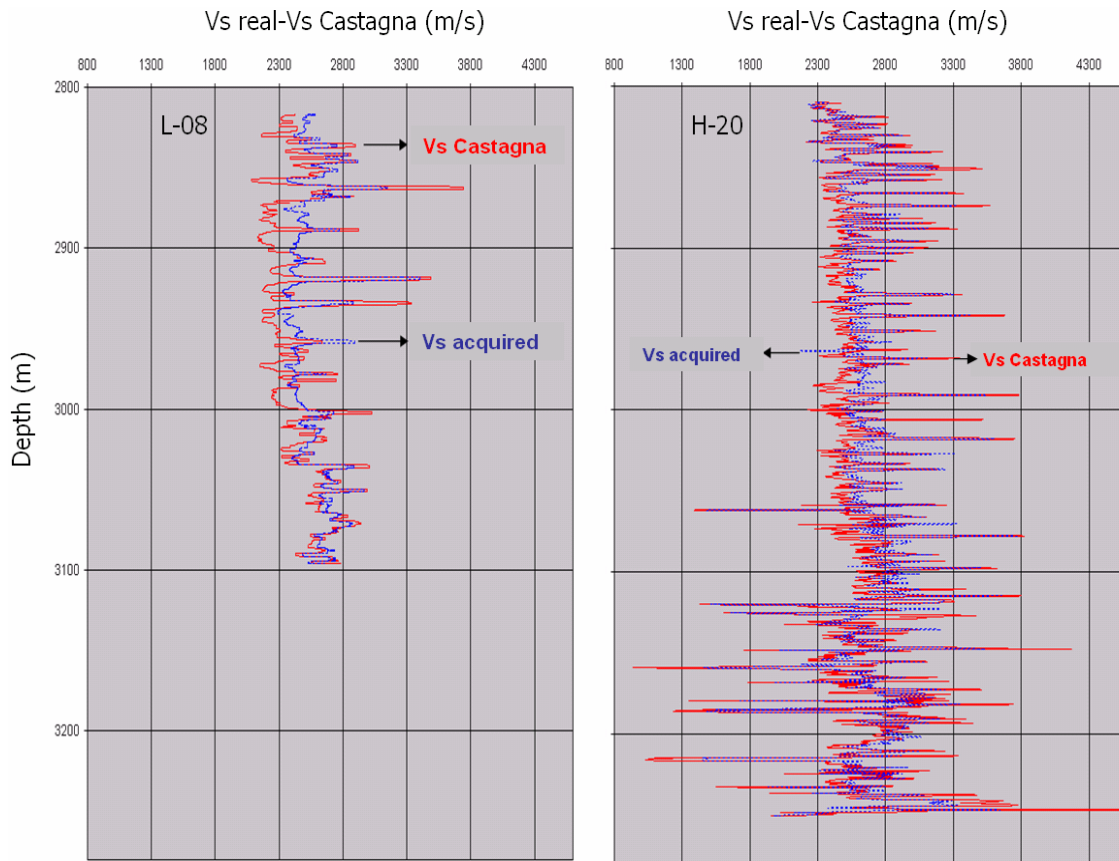


FIG. 17. Vs real and Vs Castagna versus depth (well L-08 and H-20), showing the Avalon unit.

## CONCLUSIONS

$V_p$  and  $V_s$  generally decrease with total porosity; the decrease in  $V_s$  is well correlated with porosity. We observed some negative porosity that could be indicative of calcite lime in the matrix “ $2710 \text{ kg/m}^3$ ”.

$V_p/V_s$  keep a constant range of values (1.5-2.3 for the Avalon sandstone), with total porosity.

There are some data on the top of the well that do not behave similarly to the other data. This could be the effect of casing.

Castagna is better predictor for  $V_s$  than Faust  $V_s$ . Castagna experiences difficulty predicting  $V_s$  in the limestone zone.

Typically, the Faust relation provides a reasonable prediction for  $V_s$ , but for a better fit with the well data it requires a constant different from 125.3.

## **ACKNOWLEDGMENTS**

We would like to thank Louis Chabot of Veritas Geoservices, Kevin Hall with the CREWES Project, and David Emery of Husky Energy Inc., for their help during this work.

We greatly appreciate the release of log data from Husky Energy Inc. We continue to be grateful to the CREWES Project Sponsors for their support.

## **REFERENCES**

- Castagna, J.P., Batzle, M.L., and Eastwood, R.L. 1985. Relationship between compressional-wave and shear-wave velocities in clastic silicate. **50** (4), 571-581.
- Faust, L.Y. 1951. Seismic velocity as a function of depth and geologic time. *Geophysics Journal*. **16** (2), 192-206.
- Hilchie, D. W. 1989. *Advanced Well Log Interpretation*. Hilchie Press. p. 225.
- Husky Oil Operations Limited as operator, 2001, White Rose Oilfield Development Application. Volume 2: Development Plan.
- Jaramillo S.J. and Stewart, R.R. 2002. Well-log analysis of elastic properties from the White Rose oilfield, offshore Newfoundland. CREWES Research Report, **14**, Chapter 2.
- Jaramillo S.J. and Stewart, R.R. 2003. Petrophysical relationships derived from well logs in the White Rose oilfield, offshore Newfoundland". CSEG/CSPG Extended Abstract.
- Western Atlas International Inc. 1992. *Introduction to wirelog analysis*. Western Atlas logging services. Houston, Texas. 312 p.

## **WEB PAGES**

- Geography Network, 2002. <http://www.geographynetwork.com/>
- Husky Energy, 2000. <http://www.huskywhiterose.com/>